

Relativistic Effects on Bonding in Cationic Transition-Metal–Carbene Complexes: A Density-Functional Study

Christoph Heinemann, Roland H. Hertwig, Ralf Wesendrup, Wolfram Koch,* and Helmut Schwarz*

Contribution from the Institut für Organische Chemie der Technischen Universität Berlin, Strasse des 17. Juni 135, D-10623 Berlin, Germany

Received April 25, 1994[Ⓢ]

Abstract: Nonrelativistic and quasirelativistic density-functional calculations have been performed aimed at investigating structures and bonding in the cationic methylene complexes MCH_2^+ of nickel, palladium, platinum, iridium, and gold. Relativistic effects on the bond dissociation energies of these complexes amount to +7, +15, +51, –3, and +66 kcal/mol, respectively. The influence of relativity on bond energies is analyzed in detail and discussed in terms of the s-orbital stabilization and d-orbital destabilization. The relativistic contraction of the $M^+–CH_2$ bond is found to be small for the group 10 metals and iridium but significant for gold.

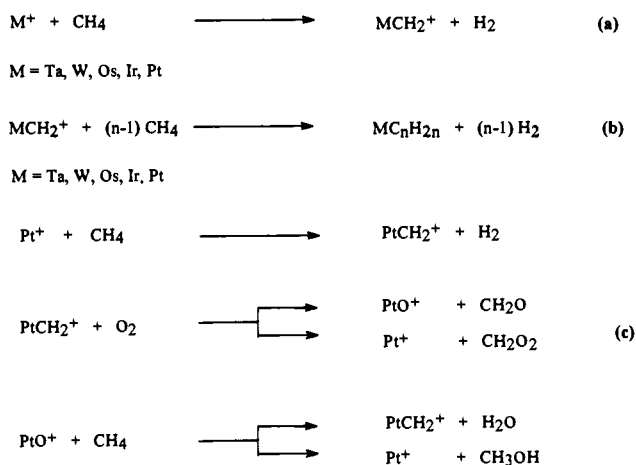
Introduction

The activation of methane constitutes an important and vivid subject of organometallic and catalytic research.^{1,2} Considerable progress in this field has been made by Beauchamp and Irikura, who reported that “bare” third-row transition-metal cations M^+ ($M = Ta, W, Os, Ir, Pt$) react exothermically with CH_4 to form the cationic carbene complexes MCH_2^+ (Scheme 1, reaction a), which in subsequent reaction steps (reaction b) afford C–C coupling reactions with up to five additional molecules of methane.³

From the point of view of catalysis, the cationic metal–carbene complexes MCH_2^+ have an interesting potential as model systems for the mechanistic study of the intrinsic reactivity of organometallic catalysts. The Pt^+ -mediated catalytic oxidation of methane by O_2 (reaction c) may serve as a recent example; here, the cationic platinum carbene $PtCH_2^+$, as formed by reaction a, constitutes a key intermediate.⁴

As an addition to the growing body of information about the intrinsic reactivity of first-, second-, and third-row transition-metal ions with hydrocarbons in the gas phase,⁵ this study

Scheme 1



addresses the question why especially the heavy third-row transition-metal cations, in contrast to their lighter homologues, are capable of bringing about methane activation. In the present article we will focus on an analysis of the bond dissociation energies (BDEs) of the cationic carbene complexes MCH_2^+ since reaction a, the initial step in the C–C coupling as well as catalytic oxidation processes, does only proceed exothermically if the bond dissociation energy of the metal cation to triplet ground state methylene exceeds 111 kcal/mol.⁶

An accurate theoretical treatment of heavy transition metals has to take into account that the relativistic motion of the inner-shell electrons (for example, the speed of a 1s electron in the hydrogen-like Pt^{77+} ion amounts to 56.9% of the speed of light in vacuum^{7d}) affects the chemically relevant valence electron distribution in atoms and molecules.⁷ This has an influence on physicochemical properties as diverse as bond lengths, ionization energies, magnetic resonance parameters, and color. The principal aim of this study is to evaluate the relativistic effects

[Ⓢ] Abstract published in *Advance ACS Abstracts*, December 1, 1994.

(1) Recent reviews: (a) Schwarz, H. *Angew. Chem., Int. Ed. Engl.* **1991**, 30, 820. (b) Fox, J. M. *Catal. Rev.-Sci. Eng.* **1993**, 35, 169.

(2) Recent reports on methane activation: (a) Ashcroft, T.; Cheetham, A. K.; Foord, J. S.; Green, M. L. H.; Grey, C. P.; Murrell, A. J.; Vernon, P. D. F. *Nature* **1990**, 334, 319. (b) Stojka, Z.; Herman, R. G.; Klier, K. *J. Chem. Soc., Chem. Commun.* **1991**, 185. (c) Capitán, M. J.; Malet, P.; Centeno, M. A.; Muñoz-Páez, A.; Carrizos, I.; Odriozola, J. A. *J. Phys. Chem.* **1993**, 97, 9233. (d) Catalytic conversion of CH_4 to CH_3OH has been listed as one of the ten challenges for catalysis: *Chem. Eng. News* **1993**, May 31, 27. (e) Lin, M.; Sen, A. *Nature* **1994**, 368, 613.

(3) (a) Irikura, K. K.; Beauchamp, J. L. *J. Am. Chem. Soc.* **1989**, 111, 75. (b) Irikura, K. K.; Beauchamp, J. L. *J. Am. Chem. Soc.* **1991**, 113, 2769. (c) Irikura, K. K.; Beauchamp, J. L. *J. Phys. Chem.* **1991**, 95, 8344. (d) The reaction of Ta^+ with CH_4 has also been investigated in: Buckner, S. W.; MacMahon, T. J.; Byrd, G. L.; Freiser, B. S. *Inorg. Chem.* **1989**, 28, 3511.

(4) Wesendrup, R.; Schröder, D.; Schwarz, H. *Angew. Chem., Int. Ed. Engl.* **1994**, 33, 223.

(5) Recent reviews: (a) Armentrout, P. B. *Annu. Rev. Phys. Chem.* **1990**, 41, 313. (b) Eller, K.; Schwarz, H. *Chem. Rev.* **1991**, 91, 1121. (c) Weishaar, J. C. *Acc. Chem. Res.* **1993**, 26, 213. For the recently explored reactivity of lanthanide cations, see: (d) Schilling, J. B.; Beauchamp, J. L. *J. Am. Chem. Soc.* **1988**, 110, 15. (e) Yiu, W. Y.; Marshall, A. G.; Marçalo, J.; Pires de Matos, A. *J. Am. Chem. Soc.* **1994**, 116, 8666. (f) Cornehl, H. H.; Heinemann, C.; Schröder, D.; Schwarz, H. *Organometallics*, in press.

(6) Lias, S. G.; Bartmess, J. E.; Lieberman, J. F.; Holmes, J. L.; Levin, R. D.; Mallard, W. G. *J. Phys. Chem. Ref. Data* **1988**, 17, Suppl. 1.

(7) (a) Balasubramanian, K.; Pitzer, K. S. *Adv. Chem. Phys.* **1987**, 67, 287. (b) Pyykkö, P. *Chem. Rev.* **1988**, 88, 563. (c) van Wezenbeek, E. M. Ph.D. Thesis, Vrije Universiteit Amsterdam, 1992. (d) Pisani, L.; André, J.-M.; André, M.-C.; Clementi, E. *J. Chem. Educ.* **1993**, 70, 894.

on the bond energies in cationic transition-metal carbene complexes. Employing density functional theory (DFT)⁸ we compare the electronic ground states of these species (i) along the Ni, Pd, Pt triad (in which all cations have a $(n-1)d^9 2D$ ground state) and (ii) for the third-row transition metals Ir, Pt, and Au, where relativistic effects are expected to be most prominent. In each case, nonrelativistic and quasirelativistic (for details, see: Theoretical Methods) calculations have been performed, so that among the elements considered in this study both the absolute magnitudes and the periodic trends in relativistic effects on bonding in cationic transition-metal carbene complexes can be analyzed in detail. Furthermore, three commonly used local and non-local functionals are compared with respect to experimental results in order to collect further information on the performance of density-functional methods in the theoretical description of bare metal-ion complexes.

Recently, high-level *ab initio* calculations have been performed on a variety of MCH_2^+ species⁹⁻¹¹ and the potential energy surfaces for reaction a.¹² Generally, an extensive treatment of electron correlation, using sophisticated multireference techniques^{9,10a,11} or coupled-cluster wave functions,^{10b} was found to be necessary to achieve good agreement of experimental and theoretical bond dissociation energies. On the basis of their generalized valence bond (GVB) method, Goddard and co-workers have developed a scheme that allows an intuitive interpretation of the electronic structures and bond dissociation energies in terms of intrinsic bond strengths, promotion, and exchange energies.^{11,13} In most of these previous calculations relativistic effects were only treated *en gros* by using relativistic effective core potentials (RECPs).¹⁴ A more detailed analysis, as presented below, does not only consider relativistic contributions for the sake of numerical accuracy but may further reveal how relativity influences the mechanisms of chemical bonding.

Theoretical Methods

All calculations reported in this study were carried out using the Amsterdam Density Functional (ADF) suite of programs.¹⁵ Inner-shell electrons ([He] at C, [Ar] at Ni, [Kr] at Pd, and [Xe]4f¹⁴ at Ir, Pt, and Au) were treated in the frozen core approximation,¹⁶ and the valence orbitals were expanded as linear combinations of Slater-type (STO) basis functions. Triple- ζ basis sets with two additional polarization functions on carbon and hydrogen were used throughout. All molecular and atomic energies were calculated using the local spin density approximation (LDA) with Slater's exchange functional and the

Vosko-Wilk-Nusair parametrization on the homogeneous electron gas for correlation,⁸ augmented by Beckes's¹⁷ (LDA+B) and additionally Perdew's¹⁸ (LDA+B+P) gradient corrections to the exchange-correlation potential.¹⁹ In the Kohn-Sham formulation of density functional theory⁸ minimization of the nonrelativistic (nr) functional $E^{nr}[\rho^{nr}]$ is achieved by finding a self-consistent solution to the following set of N one-electron equations

$$\left(-\frac{1}{2}\nabla^2(r) + v_N(r) + \int \frac{\rho^{nr}(r')}{|r-r'|} dr' + v_{xc}(\rho^{nr}(r), \nabla \rho^{nr}(r)) \right) \phi_i^{nr} = \epsilon_i^{nr} \phi_i^{nr} \quad (1)$$

In eq 1, v_N denotes the nuclear potential, v_{xc} the exchange-correlation potential, and ϕ_i a Kohn-Sham orbital with eigenvalue ϵ_i . All molecular geometries were optimized under C_{2v} symmetry using analytic gradients by minimizing the nonrelativistic energy functional $E_{LDA+B+P}[\rho]$ with respect to the nuclear coordinates. In addition, the M^+-CH_2 bond distances were reoptimized by a sequence of single-point calculations using the quasirelativistic approach outlined below. It has recently been shown that gradient-corrected DFT methods can give accurate binding energies for both main-group and transition-metal systems.²⁰

Relativistic effects on the electronic structures were evaluated using the quasirelativistic method due to Ziegler, Baerends, et al.²¹ In this approach, a first-order Hamiltonian, obtained from the N -electron Dirac-Coulomb operator^{7c} by a sequence of Foully-Wouthuysen transformations, is diagonalized in the space of the solutions to the zero-order (nonrelativistic) Hamiltonian. This leads to a quasirelativistic SCF procedure resulting in quasirelativistic densities $\rho^{qr}(r)$ and corresponding energies $E^{qr}[\rho^{qr}]$. In this scheme, eq 1 is transformed into

$$\left(-\frac{1}{2}\nabla^2(r) + v_N(r) + \int \frac{\rho^{qr}(r')}{|r-r'|} dr' + v_{xc}(\rho^{qr}(r), \nabla \rho^{qr}(r)) + h^1 \right) \phi_i^{qr} = \epsilon_i^{qr} \phi_i^{qr} \quad (2)$$

where h^1 denotes the sum of the relativistic Darwin- and mass-velocity operators. The quasirelativistic calculations employ atomic relativistic core densities and core potentials, generated from the auxiliary program DIRAC.¹⁵ Applications of this quasirelativistic methodology have demonstrated that it can successfully be employed to investigate relativistic effects on bonding, especially for third-row transition-metals and heavier elements for which relativistic influences on the valence density become important.²² The theoretical bond dissociation energies were obtained from separate spin-unrestricted calculations on MCH_2^+ , M^+ (in the experimental ground state, see below), and triplet CH_2 , respectively. Spin-orbit effects (LS coupling) on the bond energies are not taken into account in the present one-component scheme; however we stress that for a discussion of the full adiabatic potential energy surfaces and the reaction kinetics of processes such as reaction a (see Scheme 1) spin may no longer be a good quantum number.^{5a,12e} For a very accurate calculation of bond energies the significance of spin-orbit effects can of course not be ignored. For example, the 2D term of Pt^+ is split into two components ($^2D_{3/2}$ and $^2D_{1/2}$) by spin-orbit effects, and the same applies for the corresponding cationic carbene complex $PtCH_2^+$ (2A_1). Accordingly, a maximum error of 1 eV ($^2D_{3/2}/^2D_{1/2}$ splitting of Pt^+ ²⁷) may follow from the omission of spin-orbit

(8) Parr, R. G.; Yang, W. *Density Functional Theory of Atoms and Molecules*; Oxford University Press: New York, 1989.

(9) (a) Alvarado-Swaisgood, A. E.; Harrison, J. F. *J. Phys. Chem.* **1985**, *89*, 2517. (b) Alvarado-Swaisgood, A. E.; Harrison, J. F. *J. Phys. Chem.* **1988**, *92*, 2757.

(10) (a) Bauschlicher, C. W.; Partridge, H.; Sheehy, J. A.; Langhoff, S. R.; Rosi, M. *J. Phys. Chem.* **1992**, *96*, 6969. (b) Bauschlicher, C. W.; Partridge, H.; Scuseria, G. E. *J. Chem. Phys.* **1992**, *97*, 7471.

(11) Irikura, K. K.; Goddard, W. A., III *J. Am. Chem. Soc.* **1994**, *116*, 8733.

(12) (a) Musaev, G. D.; Morokuma, K.; Koga, N.; Nguyen, K. A.; Gordon, M. S.; Cundari, T. R. *J. Phys. Chem.* **1993**, *97*, 11435. (b) Musaev, D. G.; Koga, N.; Morokuma, K. *J. Phys. Chem.* **1993**, *97*, 4064. (c) Musaev, D. G.; Morokuma, K. *Isr. J. Chem.* **1993**, *33*, 307. (d) Blomberg, M. R. A.; Siegbahn, P. E. M.; Svensson, M. *J. Phys. Chem.* **1994**, *98*, 2062. (e) Perry, J. K.; Ohanessian, G.; Goddard, W. A. *Organometallics* **1994**, *13*, 1870.

(13) (a) Carter, E. A.; Goddard, W. A., III *J. Phys. Chem.* **1984**, *88*, 1485. (b) Carter, E. A.; Goddard, W. A., III *J. Am. Chem. Soc.* **1986**, *108*, 2180. (c) Carter, E. A.; Goddard, W. A., III *J. Phys. Chem.* **1988**, *92*, 5679.

(14) (a) Ermler, W. C.; Ross, R. B.; Christiansen, P. A. *Int. J. Quantum Chem.* **1991**, *40*, 829. (b) Stevens, W. J.; Krauss, M.; Basch, H.; Jasien, P. G. *Can. J. Chem.* **1992**, *70*, 612.

(15) ADF, version 1.0.2: (a) Baerends, E. J.; Ellis, D. E. *Chem. Phys.* **1973**, *2*, 71. (b) teVelde, G.; Baerends, E. J. *J. Comp. Phys.* **1992**, *99*, 84 and references cited therein.

(16) Snijders, J. G.; Baerends, E. J. *Mol. Phys.* **1977**, *33*, 1651.

(17) Becke, A. D. *Phys. Rev. A.* **1988**, *38*, 3098.

(18) Perdew, J. P. *Phys. Rev. B* **1986**, *33*, 8822.

(19) For a recent discussion of gradient-corrected exchange-correlation functionals, see: Levy, M.; Perdew, J. P. *Int. J. Quantum Chem.* **1994**, *49*, 539.

(20) (a) Becke, A. D. *J. Chem. Phys.* **1992**, *96*, 2155. (b) Ziegler, T. *Chem. Rev.* **1991**, *91*, 651. (c) Tschinke, V.; Ziegler, T. *Theor. Chim. Acta* **1991**, *81*, 65. (d) Johnson, B. G.; Gill, P. M. W.; Pople, J. A. *J. Chem. Phys.* **1993**, *98*, 5612.

(21) Ziegler, T.; Tschinke, V.; Baerends, E. J.; Snijders, J. G.; Ravenek, W. *J. Phys. Chem.* **1989**, *93*, 3050. Earlier relativistic calculations by the same authors: (a) Snijders, J. G.; Baerends, E. J. *Mol. Phys.* **1978**, *36*, 1789. (b) Snijders, J. G.; Baerends, E. J.; Ros, P. *Ibid.* **1979**, *38*, 1909. (c) Ziegler, T.; Snijders, J. G.; Baerends, E. J. *J. Chem. Phys.* **1981**, *74*, 1271. (d) Pyykkö, P.; Snijders, J. G.; Baerends, E. J. *Chem. Phys. Lett.* **1981**, *83*, 432.

(22) van Wezenbeck, E. M.; Baerends, E. J.; Snijders, J. G. *Theor. Chim. Acta* **1991**, *81*, 139.

Table 1. Structures^a and Relative Energies (in kcal/mol) for the Lowest Triplet and Singlet States of CH₂

	CH ₂ (³ B ₁)	CH ₂ (¹ A ₁)
geometries		
<i>R</i> (C–H) ^b	1.087	1.118
θ (H–C–H) ^c	138.8	103.2
relative energies		
LDA	0.0	15.0
LDA+B	0.0	10.6
LDA+B+P	0.0	16.4
exp ^{24a}	0.0	9.0

^a Calculated with the LDA+B+P functional; bond lengths in angstroms, bond angles in degrees. ^b Exp:^{24b} 1.075 (³B₁), 1.111 (¹A₁). MR-SDCI:²⁵ 1.080 (³B₁), 1.111 (¹A₁). ^c Exp:^{24b} 133.9 (³B₁), 102.0 (¹A₁). MR-SDCI:²⁵ 133.7 (³B₁), 102.1 (¹A₁).

Table 2. Nonrelativistic (nr) and Quasirelativistic (qr) *dⁿ → s¹dⁿ⁻¹* Promotion Energies for *dⁿ* Ground State Transition-Metal Cations M⁺ (in eV)

		Ni	Pd	Pt	Au
LDA	qr	1.75	3.46	1.52	2.40
	nr	2.16	4.61	3.78	5.67
LDA+B	qr	1.82	3.56	1.58	2.48
	nr	2.23	4.73	4.24	5.76
LDA+B+P	qr	1.63	3.42	1.41	2.36
	nr	2.03	4.60	4.09	5.69
exp ^d		1.08	3.19	0.78	2.29

^d From ref 27 and averaged over all *J* levels.

effects. This is within the expected error of the applied approximate density-functional^{20b} scheme. Thus, for the comparative purposes of this study we stay in the one-component scheme, which treats an average of all LS-coupled states, thereby following all recent ab initio treatments of heavy-transition-metal–carbene complexes.^{10–12}

To analyze the different contributions to the binding energies, the following decomposition scheme developed by Morokuma, Ziegler, and co-workers²³ was employed: The total binding energy ΔE_B is expressed as the sum of the steric interaction ΔE_{steric} and the orbital interaction ΔE_{OI} . The former represents the energy of interaction between M⁺ and CH₂ if the determinant wave function of the MCH₂⁺ complex is simply taken as an antisymmetrized product of the unrelaxed occupied fragment orbitals of M⁺ and CH₂. It can further be split into the "classical" electrostatic interaction $\Delta E_{\text{el.stat.}}$ of the nuclear charges and the electronic charge densities plus the so-called Pauli (or exchange) repulsion ΔE_{Pauli} which is due to the antisymmetry of the total wave function. The orbital interaction term ΔE_{OI} contains all contributions arising from charge-transfer, donor–acceptor interactions and the relaxation of the individual fragments due to the presence of the bonding partner. The energy analyses were carried out using M⁺ and CH₂ (in the geometry found in the MCH₂⁺ complex) as fragments.

All calculations were carried out on IBM RS/6000 Model 320H workstations. A single SCF procedure for an MCH₂⁺ molecule needed about 30 min of CPU time and 10–20 steps were usually necessary to optimize the geometries. This computational efficiency, as compared to highly correlated conventional MO methods, represents one of the appealing features of density functional theory.

Results and Discussion

(A) Fragments. In order to assess the reliability of our bond dissociation energy calculations we first present theoretical results for the building blocks of MCH₂⁺, i.e. the isolated methylene ligand and the metal cations M⁺ (see Tables 1 and 2). For CH₂ close agreement of the density-functional geometries with both experimental data²⁴ and high-level calculations²⁵ is found. In accord with earlier density-functional investigations

Table 3. Geometries^a for Cationic Transition-Metal–Carbene Complexes MCH₂⁺

	NiCH ₂ ⁺	PdCH ₂ ⁺	PtCH ₂ ⁺	IrCH ₂ ⁺	IrCH ₂ ⁺	AuCH ₂ ⁺
state	² A ₁	² A ₁	² A ₁	³ A ₁	³ A ₂	¹ A ₁
<i>R</i> (M–C)	1.733	1.871	1.849	1.868	1.844	2.153
<i>R</i> _{qr} (M–C) ^b	1.733	1.856	1.825	1.843	1.844	1.867
<i>R</i> (C–H)	1.105	1.107	1.106	1.108	1.108	1.104
θ (M–C–H)	121.7	120.4	120.2	121.6	121.2	123.7
θ (H–C–H)	116.6	119.2	119.6	116.8	117.6	112.6

^a Calculated nonrelativistically using the LDA+B+P functional; bond lengths in angstroms, bond angles in degrees. ^b M⁺–CH₂ distance reoptimized using the quasirelativistic method.

of divalent group 14 hydrides²⁶ the singlet–triplet splitting (exp: 9.0 kcal/mol for CH₂)^{24a} is overestimated in the local-density approximation (LDA) by 6 kcal/mol. The gradient correction due to Becke compensates this error to a large extent (LDA+B singlet–triplet splitting: 10.6 kcal/mol), while the addition of the Perdew functional (LDA+B+P) incorrectly increases the singlet–triplet gap to 16.4 kcal/mol.

Concerning the metal cations M⁺ with a *dⁿ* ground state configuration²⁷ (M = Ni, Pd, Pt (²D), Au (¹S)), the promotion energies to the lowest high-spin term arising from a *s¹dⁿ⁻¹* configuration²⁷ (M = Ni, Pd, Pt (⁴F), Au (³D), Ir⁺ has a ⁵F ground state deriving from the 6s¹5d⁷ configuration^{3c}) should be relevant for the present study since hybridization of the ns with the (n–1)d_{z²} orbitals (n = 4, 5, 6) occurs upon formation of the metal–carbon double bond.^{13c} The results collected in Table 2 show that for the relevant excitation processes density-functional theory is in qualitative agreement with the experimental values. However, it overestimates the *dⁿ → s¹dⁿ⁻¹* promotion energy in all cases. The bias of the current density functionals toward the *dⁿ* configurations, even if standard gradient corrections are applied, has already been noted for the first-row transition metals.^{28,30} According to a detailed analysis by Gunnarsson and Jones³⁰ it is due to an incorrect description of the 4s/3d, 3d/3d, and 3d/core exchange energies. Particularly for the elements of the second and third row the quasirelativistic treatment improves the results considerably, which is clearly due to the relativistic stabilization of s-orbitals and destabilization of d-orbitals. This relativistic effect on the *dⁿ → s¹dⁿ⁻¹* promotion energies is nearly insensitive to the choice of the functional, and the effect peaks, as expected, for Au⁺.

(B) Cationic Metal–Carbene complexes. The metal–carbon bond distances (see Table 3) in the ²A₁ ground states of the cationic carbene complexes along the Ni, Pd, Pt triad show no unexpected trends (*R*_{Ni–C} < *R*_{Pd–C} ≈ *R*_{Pt–C}) and can easily be rationalized in terms of atomic size. Our calculated nickel–carbon bond distance of 1.733 Å is somewhat smaller than the reported all-electron ACPF value of 1.790 Å,^{10a} which can be attributed to the choice of an [Ar] frozen core for the nickel fragment. Inclusion of the metal's 3s and 3p electrons in the valence space leads to a value of 1.763 Å with almost negligible effects on the bond energies (nonrelativistic BDE amounts to 106.8 (LDA), 83.9 (LDA+B), and 91.1 kcal/mol (LDA+B+P), compare Table 5). For PdCH₂⁺ and PtCH₂⁺ the LDA+B+P geometries (*R*_{Pd–C} = 1.871 Å, *R*_{Pt–C} = 1.849 Å) are in excellent agreement with earlier MCPF and GVB calculations (PdCH₂⁺: 1.867 Å^{10a} (MCPF); PtCH₂⁺: 1.860 Å (GVB)¹¹). For IrCH₂⁺ the two low-lying ³A₁ and ³A₂ states are structurally very similar to each other as well as to PtCH₂⁺, since only the occupation

(23) (a) Kiaura, K.; Morokuma, K. *Int. J. Quantum Chem.* **1976**, *10*, 325. (b) Ziegler, T.; Rauk, A. *Theor. Chim. Acta* **1977**, *46*, 1.

(24) (a) McKellar, A. R. W.; Bunker, P. R.; Sears, T. J.; Evenson, K. M.; Saykally, R. J.; Langhoff, S. R. *J. Chem. Phys.* **1983**, *79*, 5251. (b) Bunker, P. R.; Jensen, P. *J. Chem. Phys.* **1988**, *89*, 1327.

(25) Comeau, D. C.; Shavitt, I.; Jensen, P.; Bunker, P. R. *J. Chem. Phys.* **1989**, *90*, 6491.

(26) Selmani, A.; Salahub, D. R. *J. Chem. Phys.* **1988**, *89*, 1529.

(27) Moore, C. E. *Atomic Energy Levels*; National Standard Reference Data Series, National Bureau of Standards, NSRDS-NBS 35, Washington, D.C., 1971.

(28) Ziegler, T.; Li, J. *Can. J. Chem.* **1994**, *72*, 783.

(29) Fisher, E. R.; Armentrout, P. B. *J. Phys. Chem.* **1990**, *94*, 1674.

(30) Gunnarsson, O.; Jones, R. O. *Phys. Rev B* **1985**, *31*, 7588.

Table 4. Mulliken Population Analysis for the Quasirelativistic (qr) and Nonrelativistic (nr) Kohn–Sham Determinants of Cationic Transition-Metal Carbenes

		NiCH ₂ ⁺	PdCH ₂ ⁺	PtCH ₂ ⁺	IrCH ₂ ⁺	IrCH ₂ ⁺	AuCH ₂ ⁺
state		² A ₁	² A ₁	² A ₁	³ A ₁	³ A ₂	¹ A ₁
q(M) ^a	qr	0.71	0.99	1.25	1.26	1.27	1.31 (1.05) ^e
	nr	0.71	0.88	0.63	0.75	0.75	0.82
q(C) ^b	qr	0.28	0.04	-0.24	-0.24	-0.21	-0.29 (-0.05) ^e
	nr	0.28	0.11	0.28	0.20	0.20	0.15
d(M) ^c	qr	8.68	8.86	8.60	7.45	7.42	9.30 (9.54) ^e
	nr	8.74	8.95	8.88	7.71	7.69	9.78
s(M) ^d	qr	0.54	0.23	0.23	0.35	0.37	0.50 (0.50) ^e
	nr	0.47	0.21	0.47	0.53	0.54	0.40

^a Charge of the metal atom. ^b Charge of the carbon atom. ^c Population of the metal d-orbitals. ^d Population of the metal s-orbitals. ^e Values for AuCH₂⁺ refer to the optimized quasirelativistic geometry. The population analysis of the quasirelativistic wave function at the nonrelativistic geometry is given in parentheses. In all other cases, the changes in the orbital occupations due to reoptimization of the geometries are negligible.

pattern in the nonbonding metal orbitals is different. Inclusion of the quasirelativistic terms does not affect the metal–carbon distances in NiCH₂⁺ and IrCH₂⁺ (³A₂) but leads to a small contraction of the M⁺–CH₂ bond lengths of PdCH₂⁺ (-0.010 Å), PtCH₂⁺ (-0.025 Å), and IrCH₂⁺ (³A₁, -0.025 Å).

Compared to these cases, AuCH₂⁺ (¹A₁) is distinctly different. In the nonrelativistic case, formation of a covalent Au⁺–CH₂ double bond would involve the energetically unfavorable (see Table 2) ³D term of Au⁺. Consequently, the nonrelativistically optimized AuCH₂⁺ geometry exhibits a relatively long metal–carbon bond distance of 2.153 Å and a smaller H–C–H valence angle, from which one may infer the picture of a more electrostatic interaction between the singly charged Au⁺ ion and a more singlet-like methylene moiety. A similar conclusion was drawn by Irikura and Goddard,¹¹ who reported a GVB bond distance of 2.034 Å for the AuCH₂⁺ species using relativistic pseudopotentials. However, inclusion of the quasirelativistic terms in the DFT scheme reduces the atomic excitation energy dramatically (see Table 2), thus rendering a more covalent interaction possible. Consequently, the quasirelativistic method yields a shorter Au⁺–CH₂ bond length of 1.867 Å. The relativistic bond shortening (-0.286 Å) is considerably higher than for the other cationic carbene complexes because the electronic situation is different in the nonrelativistic and the quasirelativistic treatments, respectively.³¹ At the quasirelativistic level, the geometries of all third-row MCH₂⁺ species are now very similar and give no indication for qualitative differences in the electronic structures of these molecules.

This view is substantiated by the population analyses given in Table 4. For PtCH₂⁺ and the two very similar triplet states of IrCH₂⁺ the quasirelativistic treatment increases the charge on the metal considerably (+0.6e) which changes the polarity of the metal–carbon double bond resulting in a net electron transfer from the metal to the methylene fragment. This indicates strong covalent interactions through the metal d-orbitals which are destabilized upon inclusion of the relativistic terms. As expected, NiCH₂⁺ shows only small relativistic effects on the electron distribution and, in accord with the multireference ACPF wave function,^{10a} net charge transfer from CH₂ to the metal cation. From the population analyses one may infer that this species has some similarity with a hypothetical “nonrelativistic” cationic platinum carbene. Finally, PdCH₂⁺ occupies an intermediate position with a modest relativistic effect on the

charge distribution and small overall charge transfer from the CH₂ fragment to the metal cation.

Compared to IrCH₂⁺ and PtCH₂⁺, the nonrelativistic wave function of the cationic gold carbene yields a Mulliken charge closer to one, consistent with a less covalent and more electrostatic interaction. Similar to the other two third-row cases the quasirelativistic charge on the metal center of AuCH₂⁺ amounts to 1.3e after the inclusion of the relativistic terms. As expected from the geometry effects, the population analysis of the quasirelativistic wave function of this species is similar to PtCH₂⁺ and IrCH₂⁺. However, at the nonrelativistically optimized geometry, the optimal orbital interaction for the formation of an Au⁺–CH₂ double bond is not yet achieved (see Table 4), which brings about the significant relativistic effect on the metal–methylene distance. Furthermore, in contrast to IrCH₂⁺ and PtCH₂⁺, the relativistic treatment *increases* the population of the Au 6s orbital from 0.4 to 0.5 (the 6s population is not sensitive to the reoptimization of the Au⁺–CH₂ distance). Relativity causes a stabilization of the 6s orbital mainly due to the first-order correction from the mass-velocity term^{7c} which decreases the interatomic “kinetic” repulsion.^{21c,d} For the case discussed here, the repulsion between the electrons in 6s and 5d₂ orbitals on the metal (which have A₁ symmetry), the 3a₁ electron of the carbene ligand and the corresponding core electrons in orbitals of A₁ symmetry is important in this respect. Since the occupation of these orbitals is smaller in the quasirelativistic than in the nonrelativistic treatment there is only a relatively small bond length contraction in PtCH₂⁺ and the two low-lying states of IrCH₂⁺. However, AuCH₂⁺ shows an *increase* in the 6s occupation upon the inclusion of relativistic terms, in accord with a more pronounced relativistic bond contraction in this system.

The theoretically predicted bond dissociation energies, calculated relative to the metal ion in its electronic ground state configuration and triplet methylene, are given in Table 5 and will be discussed in the order given there.

NiCH₂⁺: Application of the local density approximation (LDA) results in a value of 112 kcal/mol for the bond energy, which exceeds the experimental bond dissociation energy (75.2 kcal/mol)²⁹ considerably. This error is compensated by ca. 25 kcal/mol through Becke’s gradient correction to the exchange energy (LDA+B) while the Perdew correction (LDA+B+P) results in a slightly higher value of 96 kcal/mol. The same overbinding tendency for unsaturated complexes of the late 3d transition-metal cations, even if gradient-corrected functionals are employed, has recently been noted for cationic hydride complexes MH⁺²⁸ by Ziegler and Li. For an explanation, the authors referred to an overestimation of $\Delta E_{xc}^{\beta\beta}$, the exchange-correlation interaction energy between the electron on the ligand and additional nonbonding metal electrons of the same spin.²⁸ In the case of the singly-bonded cationic nickel hydride NiH⁺ the LDA+B+P bond energy exceeds the experimental value by 9 kcal/mol.²⁸ Consistently, the LDA+B+P overbinding for cationic nickel–carbene complex NiCH₂⁺, in which two valence electrons of the ligand contribute to the formation of a double bond, is approximately twice as high (16 kcal/mol in the nonrelativistic case, see Table 5).

It is instructive to interpret this overbinding effect, which is found throughout the whole study (see below), in terms of the following relation given by Carter and Goddard.^{13c}

$$\text{BDE}_{\text{actual}} = \text{BDE}_{\text{intrinsic}} - \Delta E_{\text{promotion}}(d^n \rightarrow s^1 d^{n-1}) - \Delta E_{\text{exchange loss}} \quad (3)$$

This equation splits the actual bond energy BDE_{actual} of an open-shell transition-metal complex into an “intrinsic” value (which

(31) A similar effect has been found for the Au⁺–H₂O complex: Hrušák, J.; Schröder, D.; Schwarz, H. *Chem. Phys. Lett.* **1994**, *225*, 416.

(32) Su, T.; Bowers, M. T. *Int. J. Mass Spectrom. Ion Processes* **1973**, *12*, 347.

Table 5. Calculated Quasirelativistic (qr) and Nonrelativistic (nr) Bond Dissociation Energies for Cationic Transition-Metal–Carbene Complexes (in kcal/mol)

		NiCH ₂ ⁺	PdCH ₂ ⁺	PtCH ₂ ⁺	IrCH ₂ ⁺	IrCH ₂ ⁺	AuCH ₂ ⁺
State		² A ₁	² A ₁	² A ₁	³ A ₁	³ A ₂	¹ A ₁
LDA	qr	112.1	112.3	152.0	167.3	167.9	123.4 (105.2) ^a
	nr	106.1	97.1	98.7	171.1	170.6	46.6
LDA+B	qr	88.1	83.2	119.7	140.2	140.2	90.9 (81.4) ^a
	nr	81.6	68.5	66.2	143.2	141.8	25.4
LDA+B+P	qr	95.9	92.2	130.8	146.9	146.9	101.2 (87.8) ^a
	nr	89.5	77.0	76.8	149.9	149.0	29.7
Exp.		75.2 ± 1.8 ²⁹		115 ± 4.0 ⁴	> 111	> 111	> 95 (92.4) ³⁴

^a Values for AuCH₂⁺ refer to the optimized quasirelativistic geometry. Results from the quasirelativistic calculation at the nonrelativistic geometry are given in parentheses. In all other cases, the changes of the bond dissociation energies due to reoptimization of the geometries are negligible (<1 kcal/mol).

varies smoothly along a transition-metal row¹¹), negative contributions from a necessary atomic excitation process $\Delta E_{\text{promotion}}$ (here: $d^n \rightarrow s^1 d^{n-1}$) and the loss of exchange energy $\Delta E_{\text{exchange loss}}$, which occurs when unpaired electrons on the transition-metal center are paired to ligand electrons in the formation of chemical bonds ($K_{\text{sd}} + 0.5K_{\text{dd}}$ for NiCH₂⁺, where K_{sd} and K_{dd} denote s-d and d-d exchange energies, respectively).^{13c} Since we have shown that the relevant promotion energies are generally overestimated in the employed DFT scheme (see Table 2 and discussion below) and sd- as well as dd-exchange energies of transition-metal cations are also known to be too high,³⁰ one would expect too low bond energies, given that the intrinsic bond dissociation energy is correct in the DFT scheme. However, the observed trend to overshoot the experimental bond dissociation energies suggests that the “intrinsic” contributions to the binding energies of open-shell transition-metal systems (e.g. the term $\Delta E_{\text{xc}}^{\beta\beta}$) are severely overestimated by the DFT methods.

With all functionals we find a relativistic bond strengthening of 6 kcal/mol for the ²A₁ ground state of the cationic nickel carbene which is in accord with an estimate from perturbation theory.^{10a} The relativistic decrease of the $d^9 \rightarrow s^1 d^8$ excitation energy (see Table 2) gives an explanation for the bond strengthening in the sense of eq 3.

PdCH₂⁺: A value of 83.2 kcal/mol for the bond energy of PdCH₂⁺ is found using the LDA+B method. The relative trend for the three functionals employed ($\text{BDE}_{\text{LDA}} > \text{BDE}_{\text{LDA+B+P}} > \text{BDE}_{\text{LDA+B}}$) is the same as in the NiCH₂⁺ case and is found to be general for the species considered in this study. Unfortunately, no experimental bond energy has so far been reported for PdCH₂⁺, but similar to NiCH₂⁺ the relativistic LDA+B result is 13 kcal/mol higher than the best estimate (70 ± 3 kcal/mol) based on a multireference ACPF investigation.^{10a} Thus, the Pd⁺–CH₂ bond is predicted to be ca. 5 kcal/mol weaker than the Ni⁺–CH₂ bond. The relativistic contribution is, as expected, higher (+15 kcal/mol) and accounts for 18% of the total bond dissociation energy.

PtCH₂⁺: For platinum, the third-row homologue of nickel and palladium, the relativistic bond strengthening in the Pt–CH₂⁺ complex amounts to more than 53 kcal/mol, nearly 50% of its binding energy. The quasirelativistic LDA+B treatment gives a value of 120 kcal/mol for the bond dissociation energy, which is about 10 kcal/mol higher than the multireference CI value reported recently (111 kcal/mol¹¹). Both results are close to the experimental bracketing limits of 115 ± 4 kcal/mol.⁴ Independent of the functional employed, the comparison of nonrelativistic and quasirelativistic calculations clearly indicates that due to the non-negligible relativistic contributions only the Pt⁺–CH₂ bond energy exceeds 111 kcal/mol, the thermochemical limit⁶ for making the primary step of methane activation energetically possible (see Scheme 1).

IrCH₂⁺: The case of IrCH₂⁺ is qualitatively different from those discussed above in the sense that a small *weakening* (–3

kcal/mol) of the bond is found upon the inclusion of relativistic effects. Both low-lying triplet states are nearly isoenergetic and the LDA+B functional yields a bond energy of 140 kcal/mol in the quasirelativistic treatment, which is nearly 30 kcal/mol higher than the reported multireference CI values (111 kcal/mol,¹¹ 113 kcal/mol^{12c}). However, this large error is consistent with the results described above since the Ir⁺ cation has a $6s^1 5d^7$ electronic ground state configuration. Consequently, the bond energy of IrCH₂⁺ does not profit from the overestimation of the $d^n \rightarrow s^1 d^{n-1}$ promotion energy of the cation in the sense of eq 3. Taking into account that this overestimation amounts to 0.8 eV for Pt⁺, the bond energies of these two cationic carbene complexes appear to be approximately equal, in agreement with the comparative study reported by Irikura and Goddard.¹¹

These authors have pointed out that there is a striking parallel between the rate constants k for reaction a and the bond dissociation energies of the MCH₂⁺ products along the third-row transition metals.¹¹ However, they noticed a slight deviation from the general trend between Ir⁺ and Pt⁺ for which the BDE in both cases was calculated to be 111 kcal/mol while the measured rate constant was 40% of the collision rate (k_{ADO}^{32}) for Pt⁺ and 71% for Ir⁺.^{3c} Since the density functional results are in agreement with the high-level *ab initio* calculations in that the Ir⁺–CH₂ and Pt⁺–CH₂ bond strengths are of a similar magnitude, we have redetermined the rate constants k for the reactions of thermalized Pt⁺ and Ir⁺ with methane under the conditions of Fourier-Transform ICR mass spectrometry:³³ k_{Pt} and k_{Ir} were both found as 84% of the collision rate. Thus, we note that the parallel trend in the M⁺–CH₂ bond energies and the M⁺ + CH₄ rate constants along the third-row transition metals shows no irregularities. However, it has to be stressed that the interpretation of such correlations of kinetic with thermodynamic data is not straightforward and has to be carried out with great caution.

AuCH₂⁺: In agreement with the recent comparative MRCI study by Irikura and Goddard,¹¹ the Au⁺–CH₂ bond energy is the smallest one among all systems considered in this study with a quasirelativistic LDA+B value of 90.9 kcal/mol. However, the relativistic contribution amounts to 66 kcal/mol, which is more than 70% of the total bond energy. Unfortunately, only a lower bound of 95 (or 92.4) kcal/mol can be

(33) The experiments were performed with a Spectrospin CMS 47X FTICR mass spectrometer under conditions which have been described in detail elsewhere.⁴ In brief, metal cations were generated by laser desorption/laser ionization of iridium and platinum and were transferred to the analyzer cell. After the most abundant metal isotope was isolated by using FERETS [Forbes, R. A.; Laukien, F. H.; Wronka, J. J. *Int. Mass Spectrom. Ion Processes* **1988**, *83*, 23], the ions were thermalized by collisions with pulsed-in argon and subsequently reisolated. The degree of thermalization was assumed to be complete, if no further change in reactivity occurred on increasing the number of collisions with argon. Methane was admitted to the FTICR cell at constant pressure *via* a leak valve. The pseudo-first-order rate constants were determined from the logarithmic decay of the metal-ion intensity over time and are reported with $\pm 25\%$ error.

Table 6. Decomposition^a of Nonrelativistic (nr) and Quasirelativistic (qr) Binding Energies for Cationic Transition-Metal–Carbene Complexes (in kcal/mol)

	NiCH ₂ ⁺			PdCH ₂ ⁺			PtCH ₂ ⁺		
	nr	qr	Δ ^b	nr	qr	Δ ^b	nr	qr	Δ ^b
ΔE _{Pauli repulsion}	137	137	0	176	175	-1	262	257	-5
ΔE _{el.stat.}	-95	-96	-1	-116	-119	-3	-165	-174	-9
ΔE _{steric} ^c	54	53	-1	73	69	-4	111	97	-14
orbital interaction									
ΔE _{A1} ^c	-98	-106	-8	-72	-94	-22	-90	-148	-58
ΔE _{A2} ^c	1	-1	-2	0	-1	-1	-2	0	2
ΔE _{B1} ^c	-37	-31	6	-75	-64	11	-87	-74	13
ΔE _{B2} ^c	-12	-14	-2	-4	-3	1	-11	-5	6
Σ(orbital interactions) ^c	-146	-152	-6	-151	-162	-11	-190	-227	-37
total binding energy, ΔE _B ^{c,d}	-92	-99	-7	-78	-94	-15	-79	-132	-51

^a According to the decomposition scheme developed by Morokuma and Ziegler:²³ total binding energy ΔE_B = ΔE_{steric} + Σ(orbital interactions) = ΔE_{Pauli repulsion} + ΔE_{el.stat.} + Σ(orbital interactions). ^b Difference of quasirelativistic and nonrelativistic value. ^c Including non-local corrections. ^d Relative to M⁺(d⁹) and CH₂(³B₁) in the geometry encountered in the complex.

derived from experiment.³⁴ For comparison, a value of 94 ± 3 kcal/mol has been recommended on the basis of the MRCI investigation¹¹ in which relativistic effects were taken into account by the pseudopotential method. We note that for both the geometry and dissociation energy of AuCH₂⁺ relativistic effects are far from negligible and substantiate the view^{7b} that gold is a unique element for the study of the effects of relativity on chemistry.

To analyze the different contributions to the relativistic bond strengthening in the Ni, Pd, Pt triad in more detail we present in Table 6 the results of an energy decomposition for the relativistic and nonrelativistic bond energies. It is clearly shown that the main stabilizing donor–acceptor interactions between the metal cation and the methylene fragment arise from the orbitals in the A₁ (σ-bond) and B₁ (π-bond) irreducible representations of C_{2v}. In the quasirelativistic treatment the stabilizing orbital interactions increase under A₁ symmetry and decrease under B₁. To a first approximation this can be understood as a weakening of the π-component and a strengthening of the σ-component of the double bond plus a stabilization of the s-contribution to the nonbonding metal orbitals. The increased interaction in A₁ symmetry can be traced back to the relativistic stabilization of the ns orbital which make ns/(n - 1)d_{z²} hybridization more efficient. In addition, the Pauli interaction becomes slightly less repulsive while the stabilizing electrostatic interaction increases to a small extent upon the inclusion of the relativistic terms. However, this accounts for less than 30% of the total relativistic bond strengthening effect.

In general, the relativistic enhancement of the M⁺–CH₂ binding energies (M = Ni (+7 kcal/mol), Pd (+15 kcal/mol), Pt (+52 kcal/mol), Au (+66 kcal/mol)) has an interesting parallel to the relativistic decrease of the dⁿ → s¹dⁿ⁻¹ promotion energies of the corresponding transition metal cations (Ni⁺: -0.4 eV; Pd⁺: -1.2 eV; Pt⁺: -2.7 eV; Au⁺: -3.3 eV, see Table 2). From this qualitative relation the net bond strengthening in the cationic metal carbene complexes investigated in this study can be understood in terms of eq 3 as arising from a reduction of the dⁿ → s¹dⁿ⁻¹ promotion energy of the cation due to the well-known relativistic stabilization of the metal s-orbitals and destabilization of the metal d-orbitals. In line with this view the bond dissociation energy of the cationic carbene complex

of the s¹dⁿ⁻¹ ground state Ir⁺ cation remains nearly unaffected by the relativistic corrections. Further comparative studies to probe the validity of this interpretation are underway and will be presented later in a more general context.

Conclusions

Nonrelativistic and quasirelativistic density-functional calculations on the ground states of the cationic carbene complexes of Ni, Pd, Pt, Ir, and Au show a relativistic bond strengthening in the order of +7 (NiCH₂⁺), +15 (PdCH₂⁺), +53 (PtCH₂⁺), and +66 (AuCH₂⁺) kcal/mol and a small relativistic bond weakening for IrCH₂⁺ (-3 kcal/mol). The observed trends can be understood in a one-electron picture from the metal cation dⁿ → s¹dⁿ⁻¹ promotion energies and the well-known relativistic effects on s- and d-orbital energies. Among the three functionals employed in this study the local density approximation augmented by Becke's gradient correction to the exchange energy (LDA+B) gives the closest agreement to experimental data and high-level ab initio calculations. However, the density-functional methods consistently yield too high bond energies for the systems considered in this study. Since generally LDA+B+P (which in addition to LDA+B also contains gradient corrections to the correlation functional) is regarded as the most accurate of the functionals employed in our investigation (note, however, that a straightforward definition of the "highest level of theory", similar to ab initio Hartree–Fock based methods, is not easily accomplished in DFT) one cannot exclude that the relatively good performance of the LDA+B functional in the present study profits partly from a fortunate cancellation of errors. In general, relativity affects the bond energies of cationic carbene complexes considerably and constitutes one reason for the high activity of third-row transition-metal cations in the activation of methane.

Acknowledgment. This work has benefitted from discussions with Dr. D. Schröder and Dipl.-Chem. A. Fiedler. We are grateful to Dr. K. Irikura, Prof. W. A. Goddard, Dr. J. Lie, and Prof. T. Ziegler for providing preprints of refs 11 and 28. Financial support by the Deutsche Forschungsgemeinschaft, the Fonds der Chemischen Industrie, and the Gesellschaft der Freunde der Technischen Universität Berlin, as well as a gift of transition metals from DEGUSSA AG, Hanau, are gratefully acknowledged. C.H. thanks the Fonds der Chemischen Industrie for a Kekulé Ph.D. fellowship. We thank one of the reviewers for constructive comments.

(34) Chowdhury, A. K.; Wilkins, C. L. *J. Am. Chem. Soc.* **1987**, *109*, 5336. The lower limit for the BDE(Au⁺–CH₂) of 95 kcal/mol given in this paper was derived from a minor reaction of Au⁺ with CH₃I which may be due to kinetically or electronically excited ions (see ref 11). The major reaction of Au⁺ with CH₃Br leads to a limit of 92.4 kcal/mol.